www.uv.es/virgogroup

Overview of gravitational wave modelling

José Antonio Font

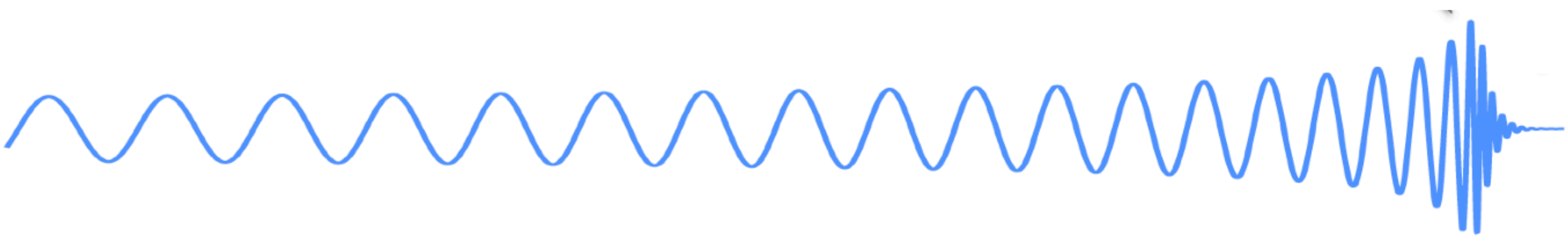

Gravitational Wave Sources

Known waveforms ⟷ Unknown waveforms

Short duration (~1s) ↕ Long duration (∞)

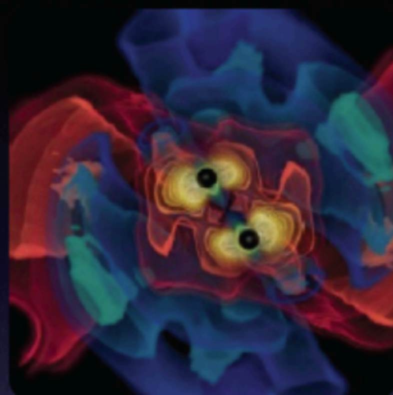

Credit: AEI, CCT, LSU

Coalescing Binary Systems

Neutron Stars, Black Holes

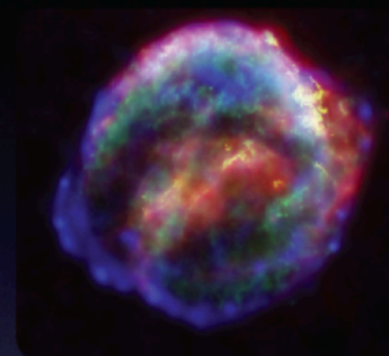

Credit: Chandra X-ray Observatory

'Bursts'

asymmetric core collapse supernovae
cosmic strings
???

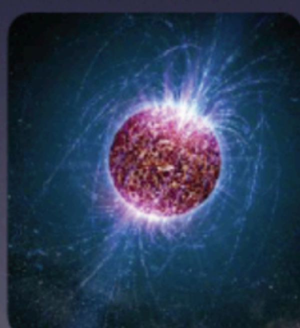

Casey Reed, Penn State

Continuous Sources

Spinning neutron stars
crustal deformations, accretion

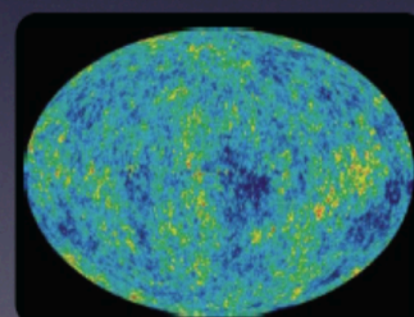

NASA/WMAP Science Team

Astrophysical or Cosmic GW background

stochastic, incoherent background

(Credit: Marie-Anne Bizouard)

Gravitational Wave Sources

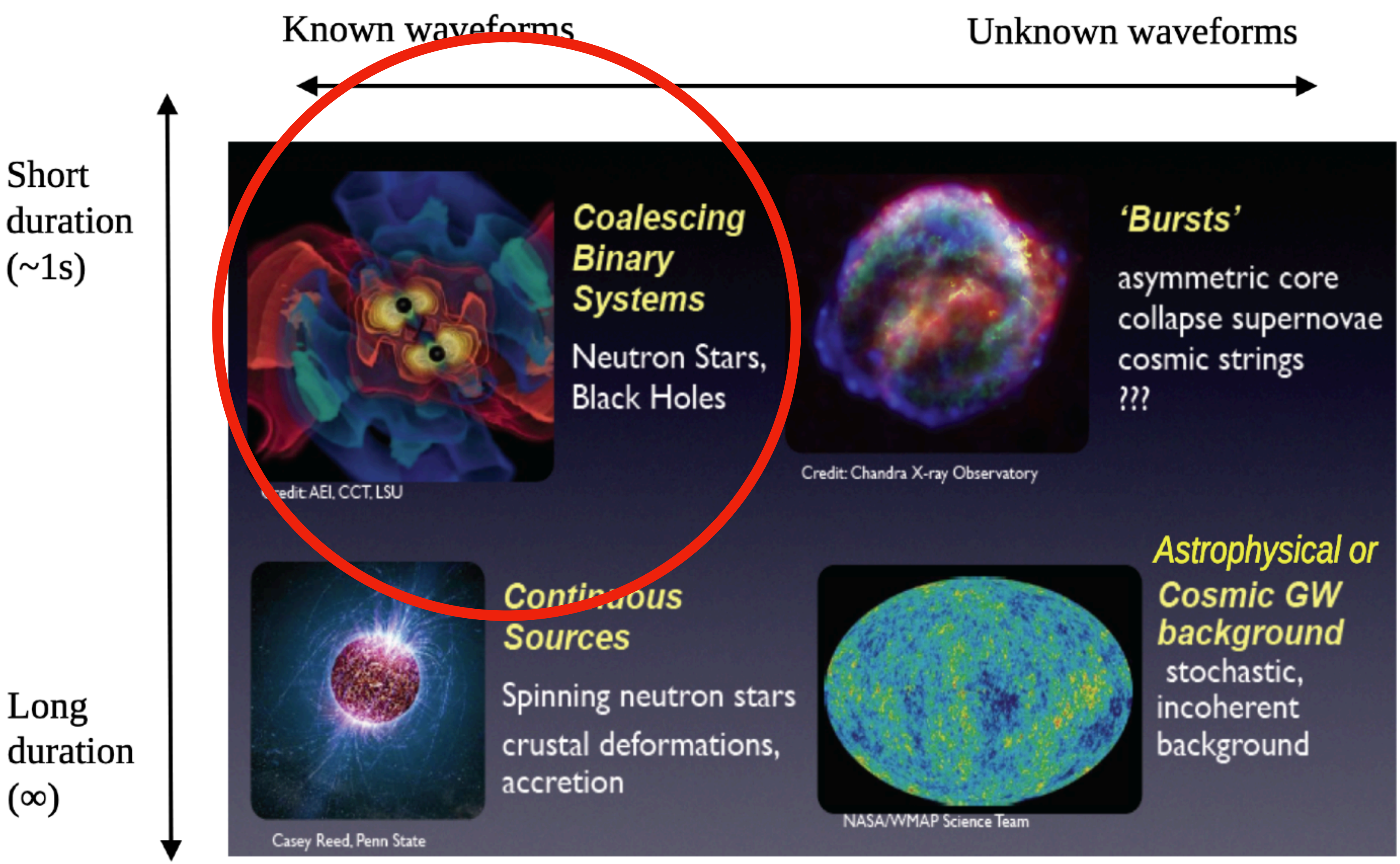

(Credit: Marie-Anne Bizouard)

GW150914

First detection!

9:50:45 UTC, 14 September 2015

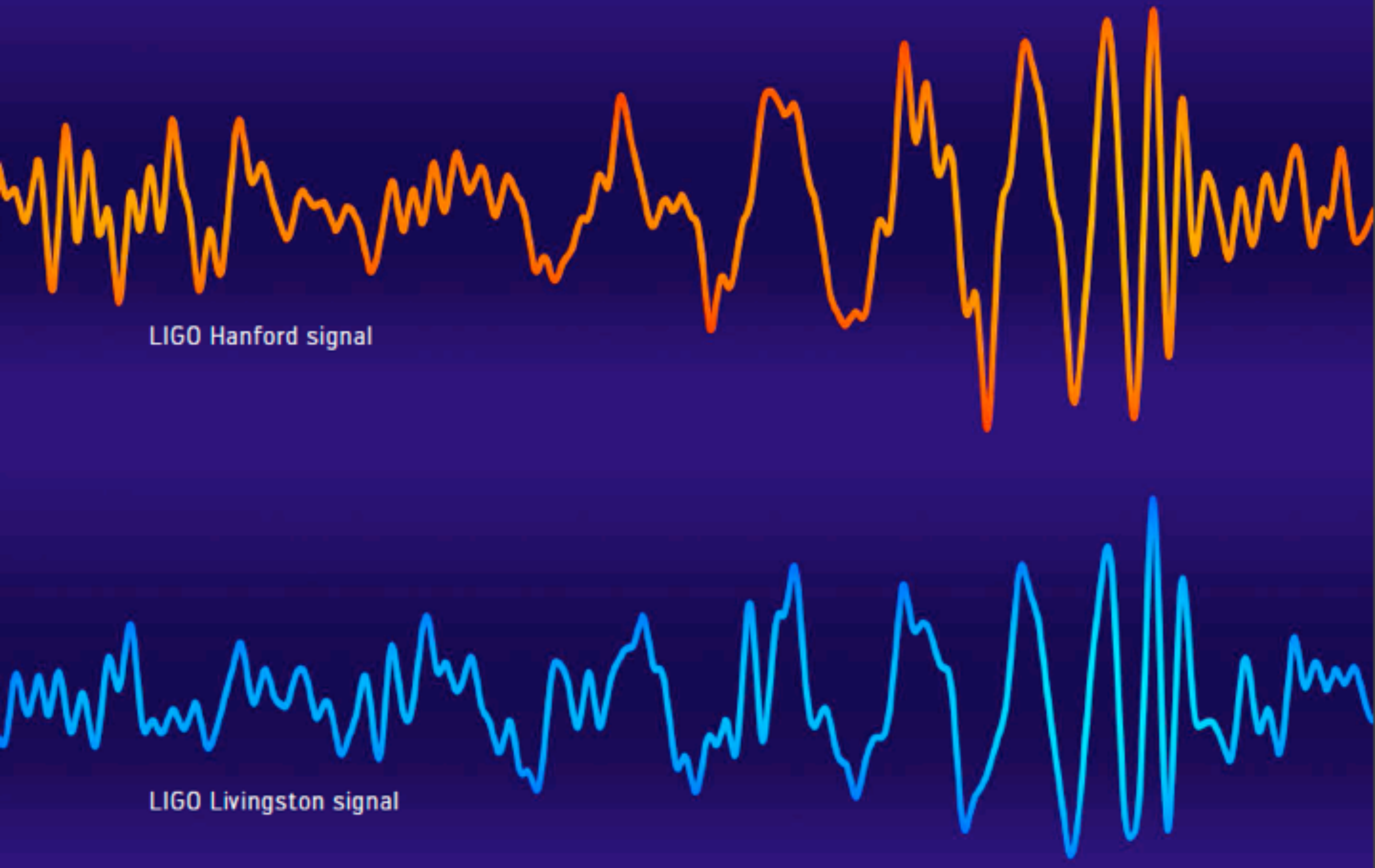

What originated GW150914? [Testing GR in the strong-field regime]

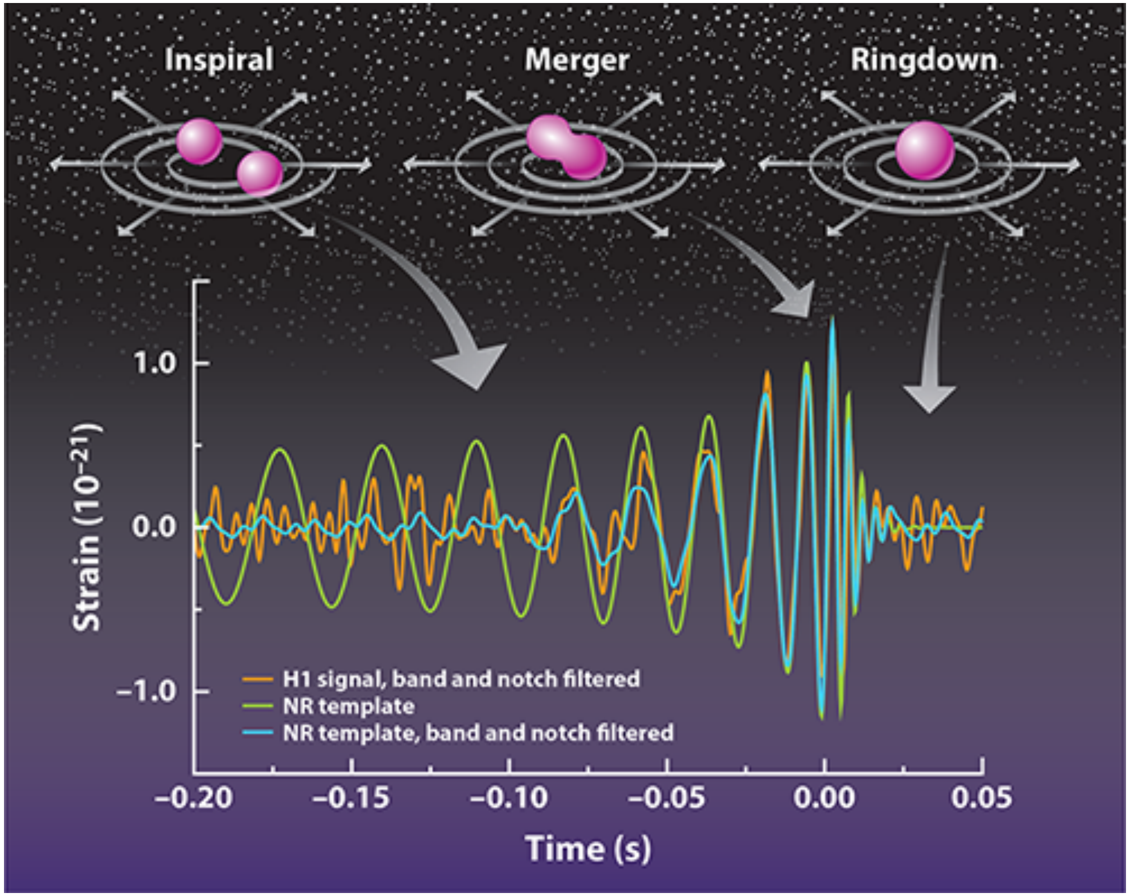

Frans Pretorius
APS/Carin Cain

Using Einstein's GR the LVK collaboration determined the theoretical framework, or "**template**", that best fit the signal. The main finding is that the **residual signal** - obtained by subtracting the template from the data - is **consistent with noise**.

GW150914 taught us how close nature follows Einstein's theory for colliding BHs.

GW observations

GWTC-1:

11 GW events from O1 & O2

Including GW150914 & GW170817

GWTC-2 & GWTC-2.1:

44 new GW events (O3a)

GWTC-3:

35 new GW events (O3b)

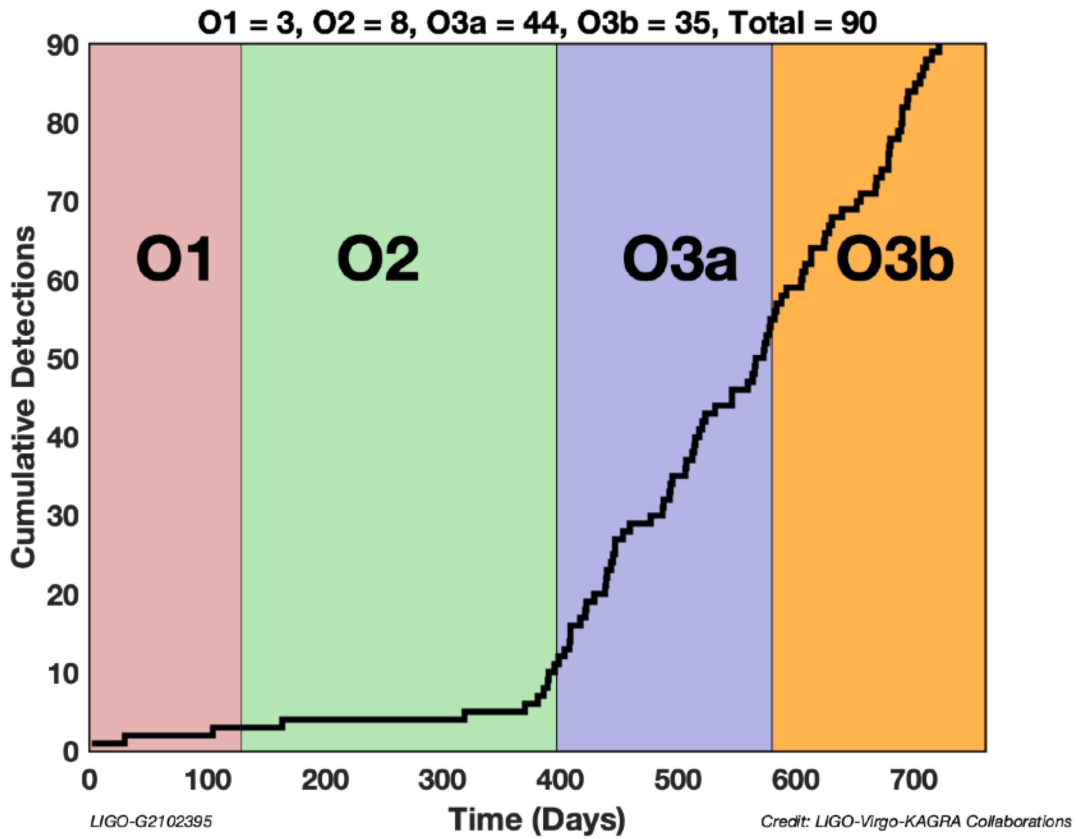

O3 detection rate ~ 1 event every 5 days

O4-O5 detection rate ~ 1-few events per day

GW observations

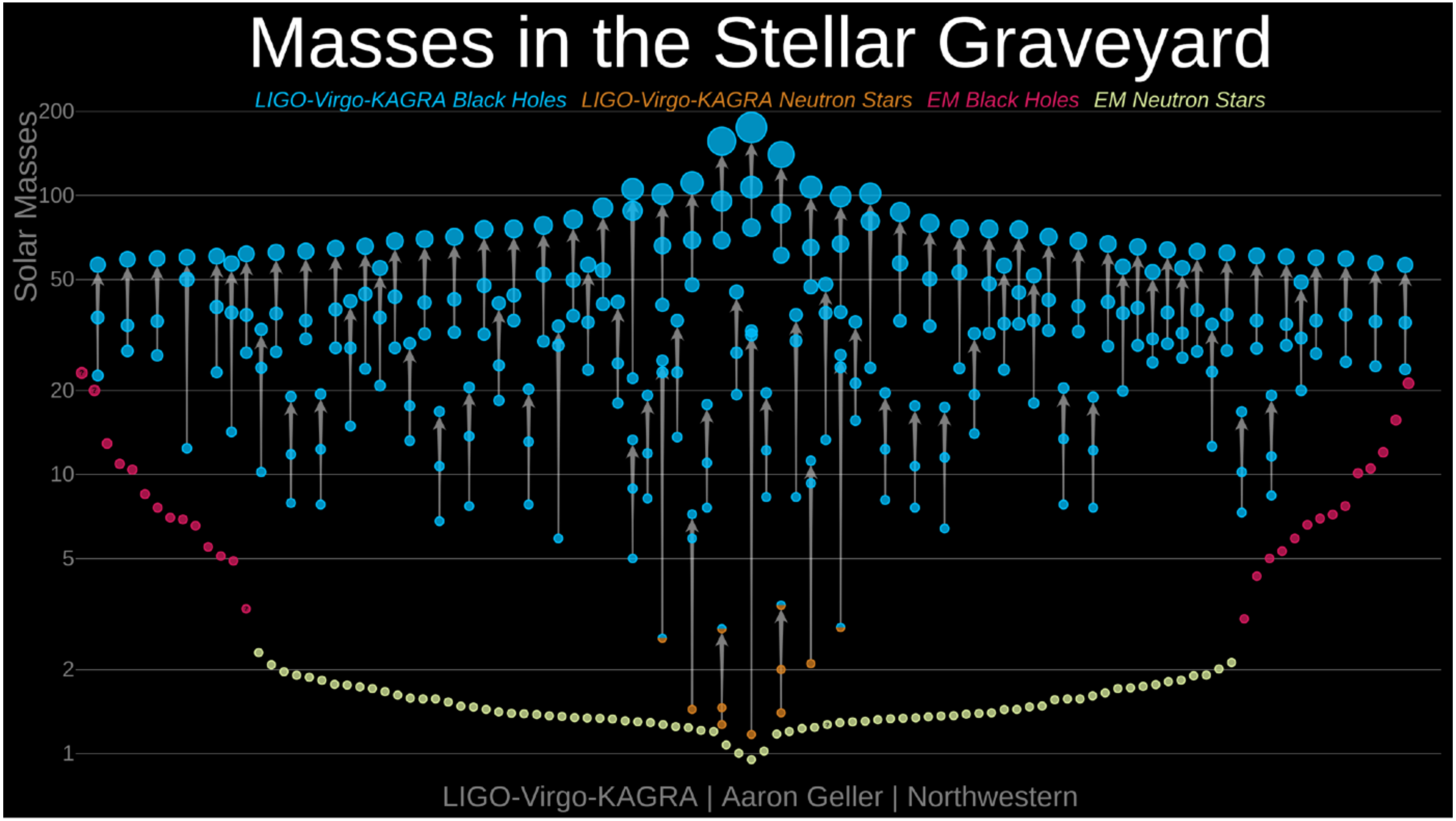

All events through end of O3 with p_astro > 0.5

3G Detectors

With ET and CE, GW observatories will leap from monitoring only the nearby Universe to surveying the entire Universe for BH mergers

Redshift reach of LIGO Voyager, ET, and CE. Shown are the redshifts for:

- BNS mergers
- BBH mergers

Assumptions:

- Madau-Dickinson SFR
- Time from binary formation to merger is 100 Myr

Most binaries merge at z~2

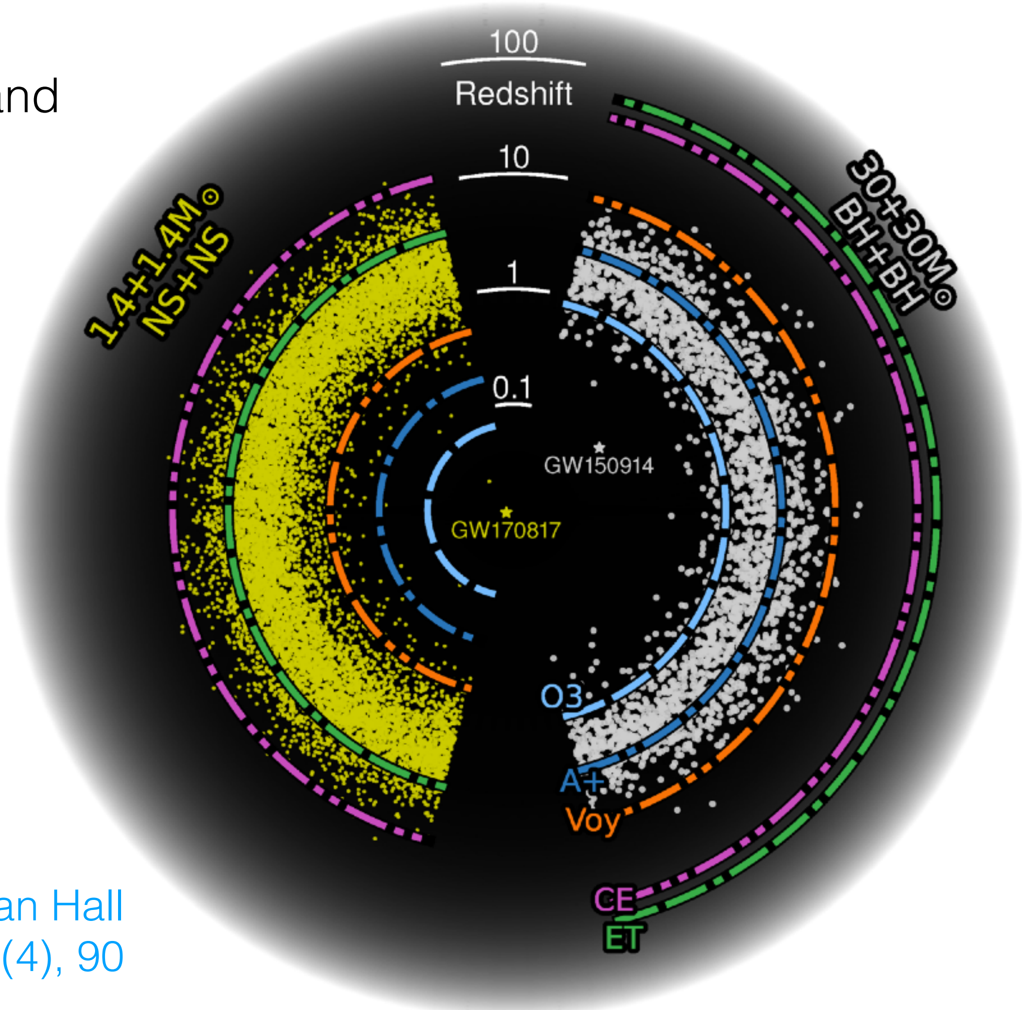

Evan Hall
Galaxies **2022**, 10(4), 90

GW observations

All events detected so far are consistent with **compact binary mergers**.

Signal “chirps” in the sensitivity band of the detector.

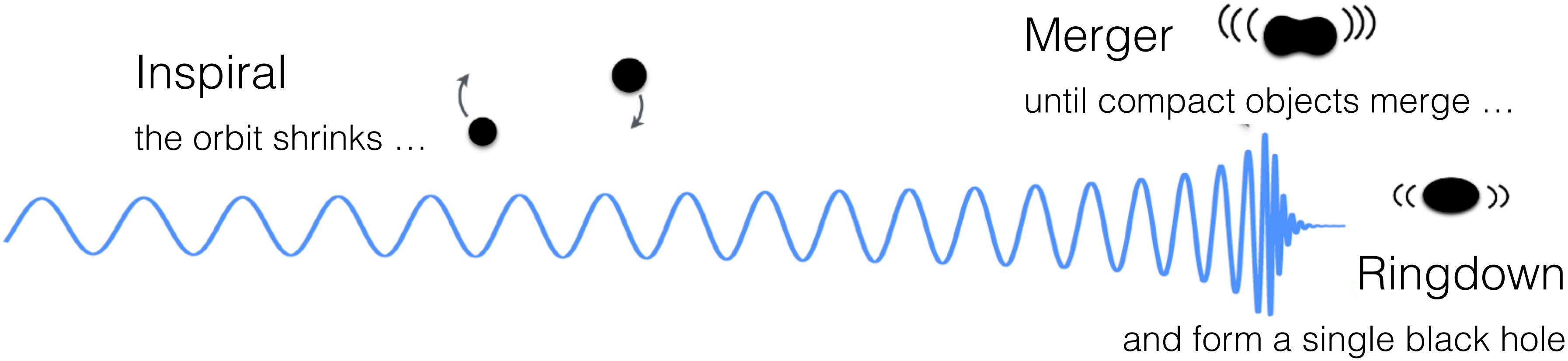

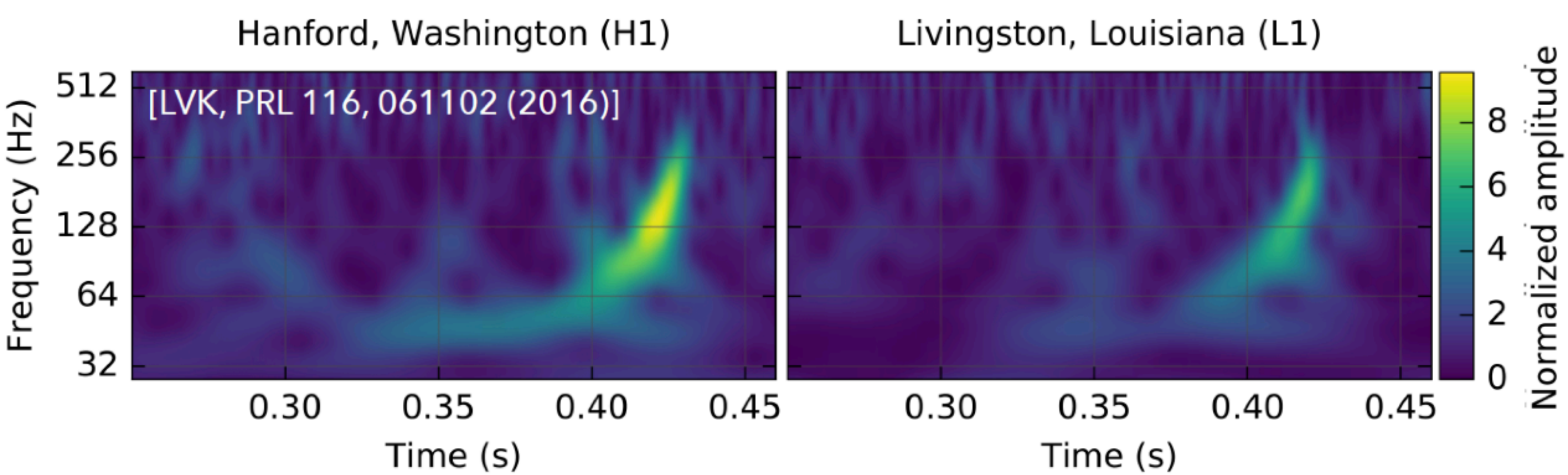

CBC sources - modelled sources

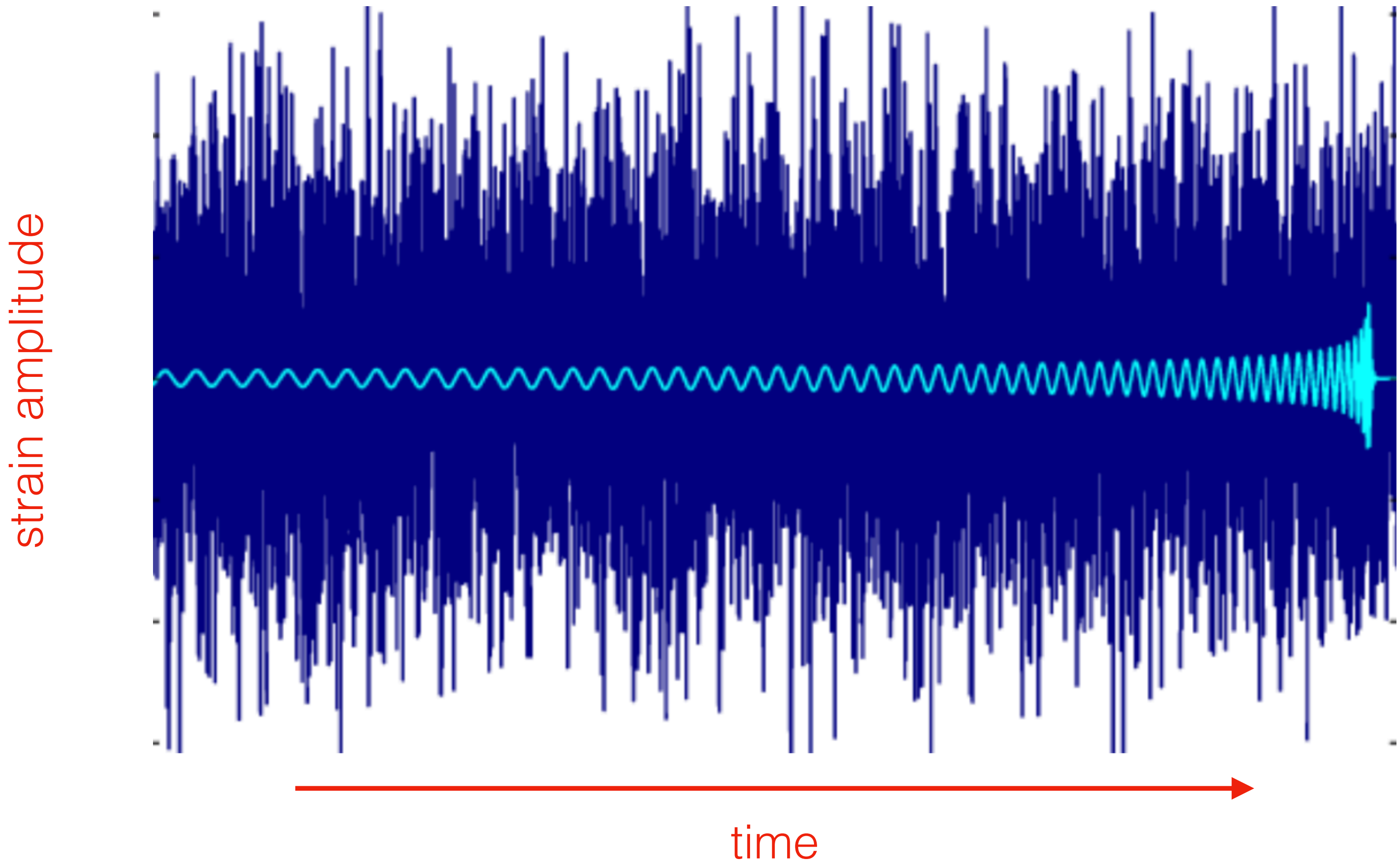

GW signal buried into noise. To dig the signal out, searches are based on **matched-filtering** using template banks from GR.

CBC waveform modelling - IMR framework

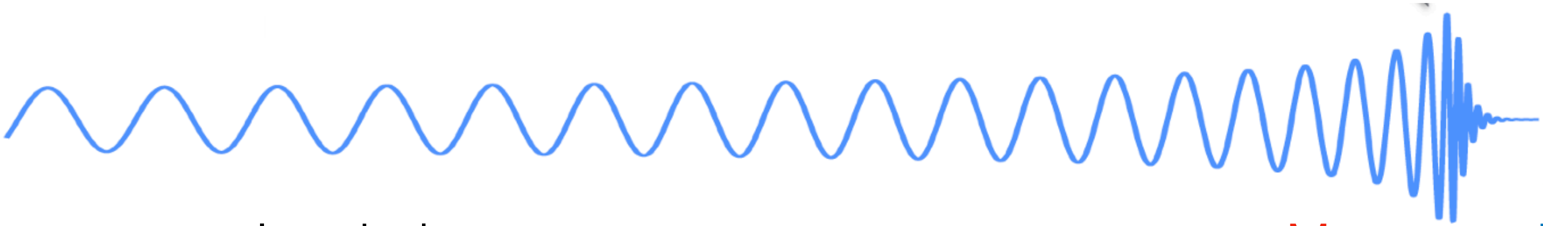

Inspiral | Merger | Ringdown

Post-Newtonian theory
Effective One-Body

[Analytical relativity]

Numerical relativity

BH perturbation theory

Huge amounts of template waveform banks required for both detection and parameter estimation. Banks **incomplete** in some regions of the parameter space (large mass ratio, precession, non QC orbits, …).

Numerical relativity is our best tool to model CBC waveforms. **But**: incomplete physics, insufficient resolution, memory and computer power limitations. Very expensive.

Synergy between numerical relativity and analytical relativity fundamental.

Numerical relativity - basic model

- Einstein's field equations $$G_{\mu\nu} \equiv R_{\mu\nu} - \frac{1}{2} g_{\mu\nu} R = 8\pi T_{\mu\nu}$$

  Formulations: BSSN, Z4, GHF (hyperbolicity).
  Methods: high-order finite differencing, (pseudo-)spectral methods.

- Hydrodynamics equations $$\nabla_\mu T^{\mu\nu} = 0 \qquad \nabla_\mu (\rho u^\mu) = 0$$

  Flux-Conservative hyperbolic formulations ("Valencia").
  Methods: high-order shock-capturing finite volume.

Current frontier:

- initial data (spins, precession, eccentric orbits) — BBH

- microphysics for thermal EOS
- magnetic fields (MRI, amplification, jet formation)
- dissipative (non ideal) fluids
- neutrino radiation transport (full Boltzmann, M1)
- nucleosynthesis (nuclear reaction network)

NS/BH - BNS

The NR BBH breakthrough

PRL **95**, 121101 (2005) PHYSICAL REVIEW LETTERS week ending 16 SEPTEMBER 2005

Evolution of Binary Black-Hole Spacetimes

Frans Pretorius[1,2,*]

[1]*Theoretical Astrophysics, California Institute of Technology, Pasadena, California 91125, USA*
[2]*Department of Physics, University of Alberta, Edmonton, AB T6G 2J1 Canada*

(Received 6 July 2005; published 14 September 2005)

We describe early success in the evolution of binary black-hole spacetimes with a numerical code based on a generalization of harmonic coordinates. Indications are that with sufficient resolution this scheme is capable of evolving binary systems for enough time to extract information about the orbit, merger, and gravitational waves emitted during the event. As an example we show results from the evolution of a binary composed of two equal mass, nonspinning black holes, through a single plunge orbit, merger, and ringdown. The resultant black hole is estimated to be a Kerr black hole with angular momentum parameter $a \approx 0.70$. At present, lack of resolution far from the binary prevents an accurate estimate of the energy emitted, though a rough calculation suggests on the order of 5% of the initial rest mass of the system is radiated as gravitational waves during the final orbit and ringdown.

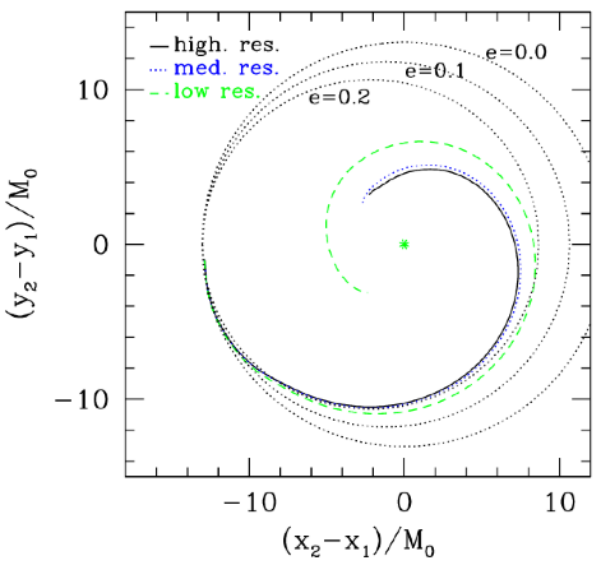

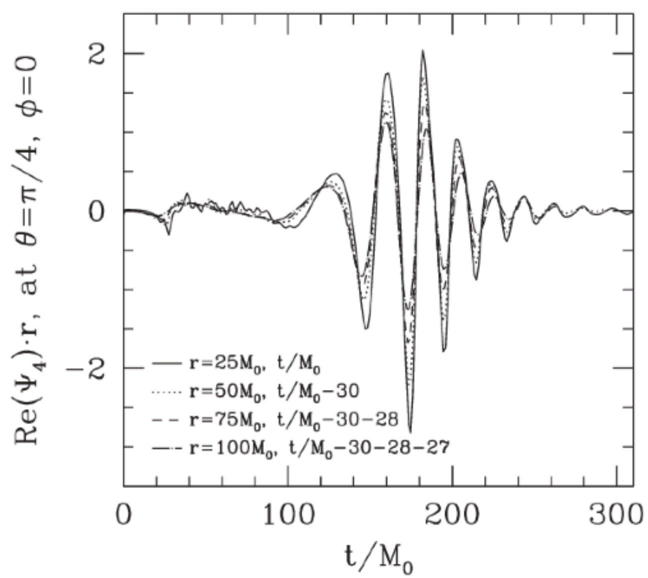

The NR BBH breakthrough

Campanelli+ PRL **96,** 111101 (2006) PHYSICAL REVIEW LETTERS week ending 24 MARCH 2006

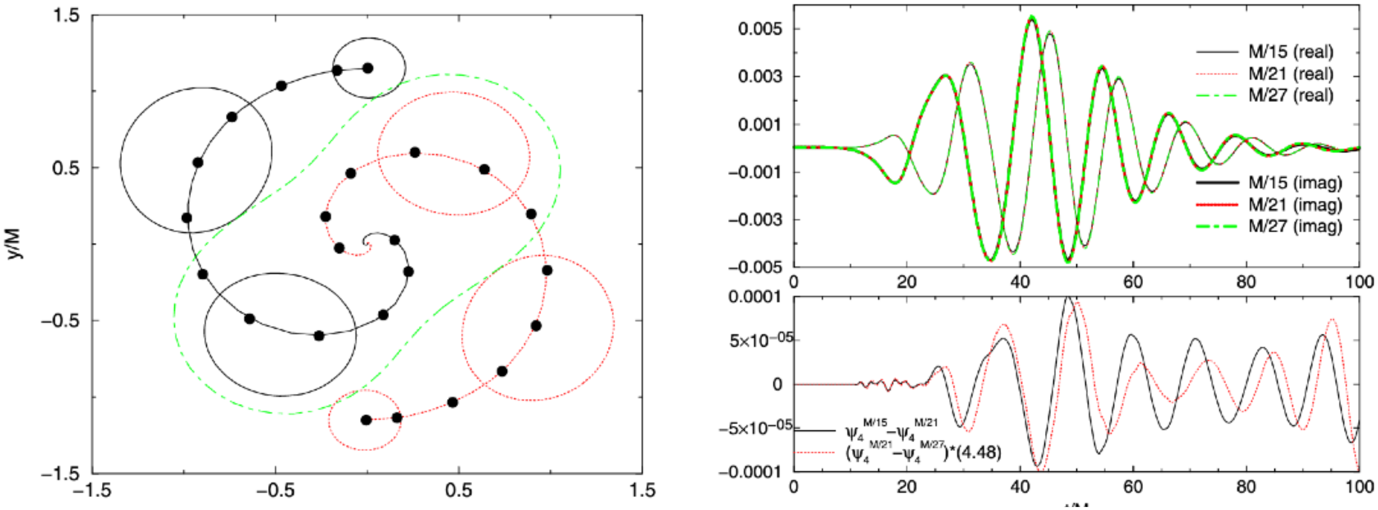

Baker+ PRL **96,** 111102 (2006) PHYSICAL REVIEW LETTERS week ending 24 MARCH 2006

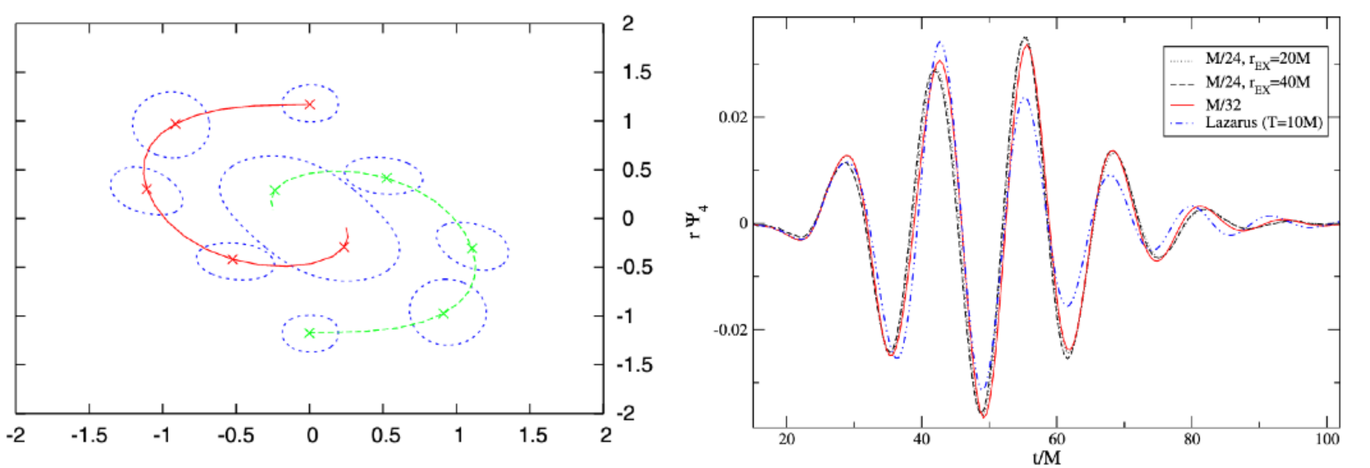

Shortly followed by many more NR groups worldwide …

The NR BBH breakthrough

1995: Pair of pants
(Head-on collision)

BBH Grand Challenge Alliance

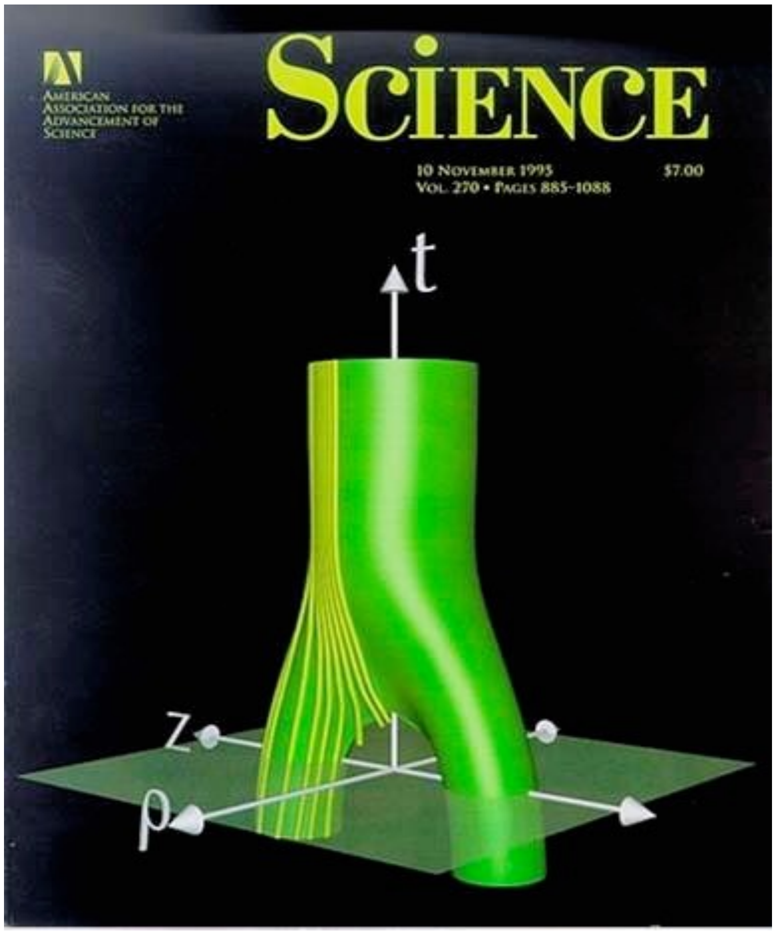

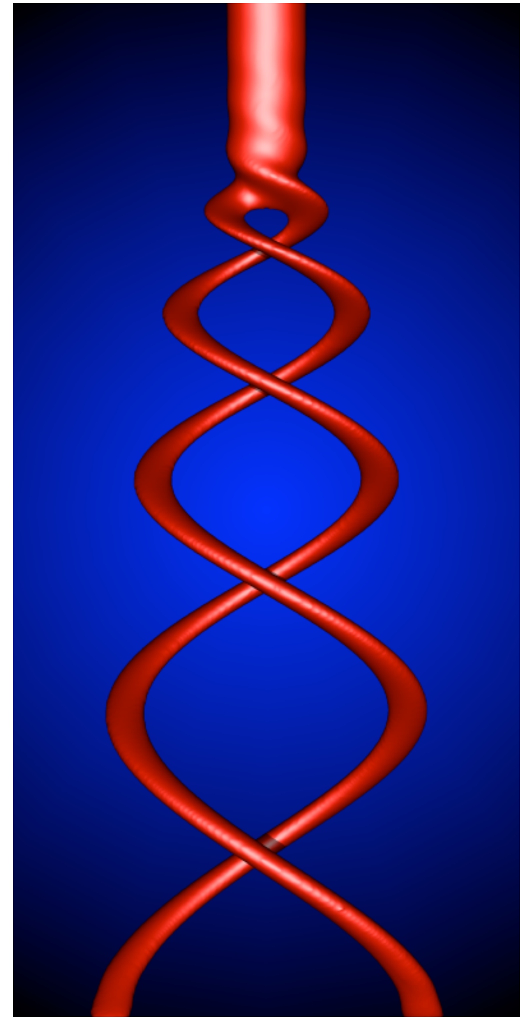

FSU-Jena Numerical Relativity Group

2007: Pair of twisted pants
(spiral & merge)

Numerical relativity - waveform catalogs

NR is now a **mature field**. Diverse **codes available**, some as open source: **`SpEC`**, **`LazEv`**, **`BAM`**, **`Einstein Toolkit`**, **`GRChombo`**, **`MayaKranc`**, etc.

Several NR groups maintain GW catalogs, e.g. the SXS Collaboration Catalog (Boyle+ 2019), the RIT Catalog (Healy & Lousto 2022), the CoRe Database (Dietrich+ 2018), etc.

Available BBH waveforms from NR simulations: O(1000)
Available BNS waveforms from NR simulations: O(100)

Despite the large number of publicly available WF from NR simulations, the **parameter space coverage still insufficient** for direct use in PE techniques.

LVK BBH detections use **O(10^6-10^7) WFs**, mostly from Analytical Relativity.

However, NR catalogs are an invaluable source of information for the **calibration** and **improvement** of semi-analytical models (see talk by Simone).

Numerical relativity - waveform catalogs

SXS (early) catalog of 174 BBH waveforms for GW astronomy (Mroué+ 2013)

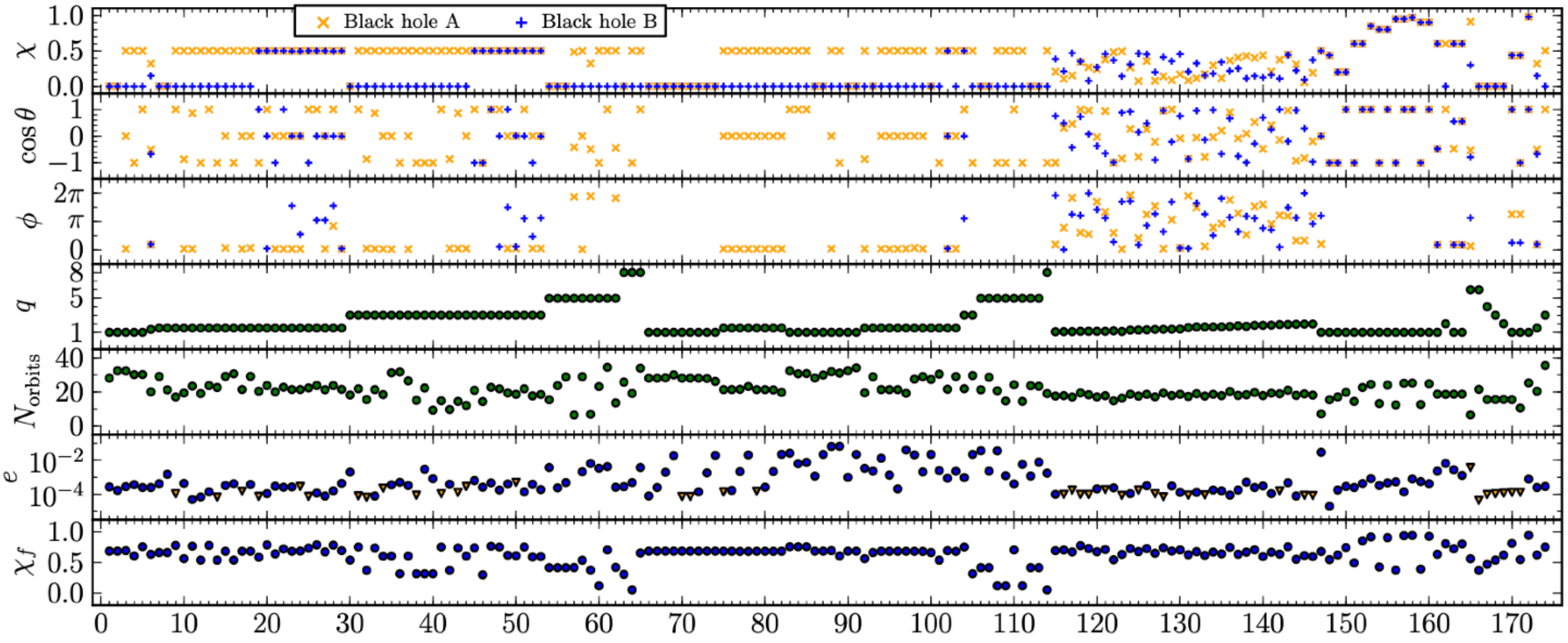

Latest SXS catalog (Boyle+ 2019) includes 2018 BBH WFs

Numerical relativity - waveform catalogs

SXS (early) catalog of 174 BBH waveforms for GW astronomy (Mroué+ 2013)

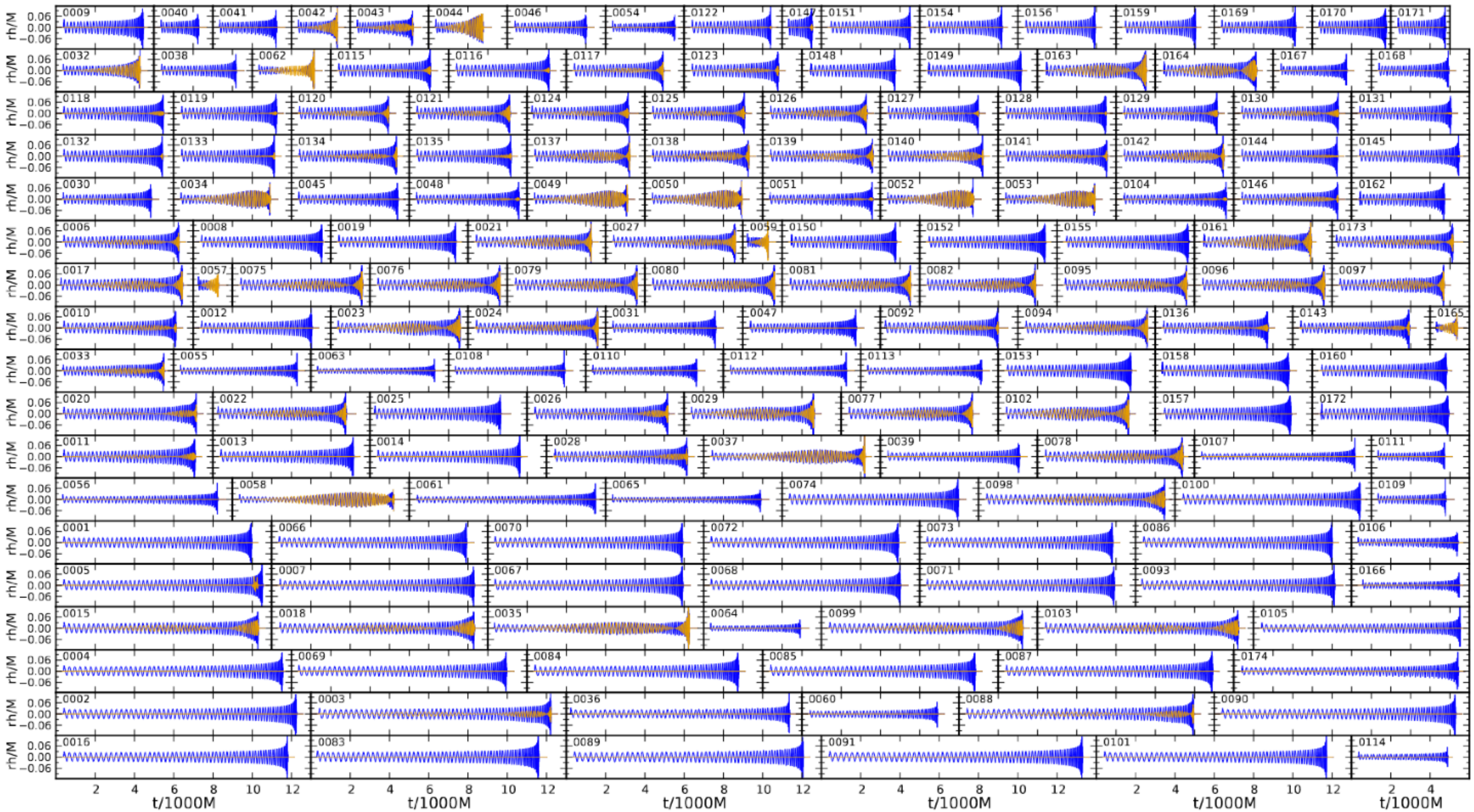

Numerical relativity - waveform catalogs

CoRe BNS database (www.computational-relativity.org)

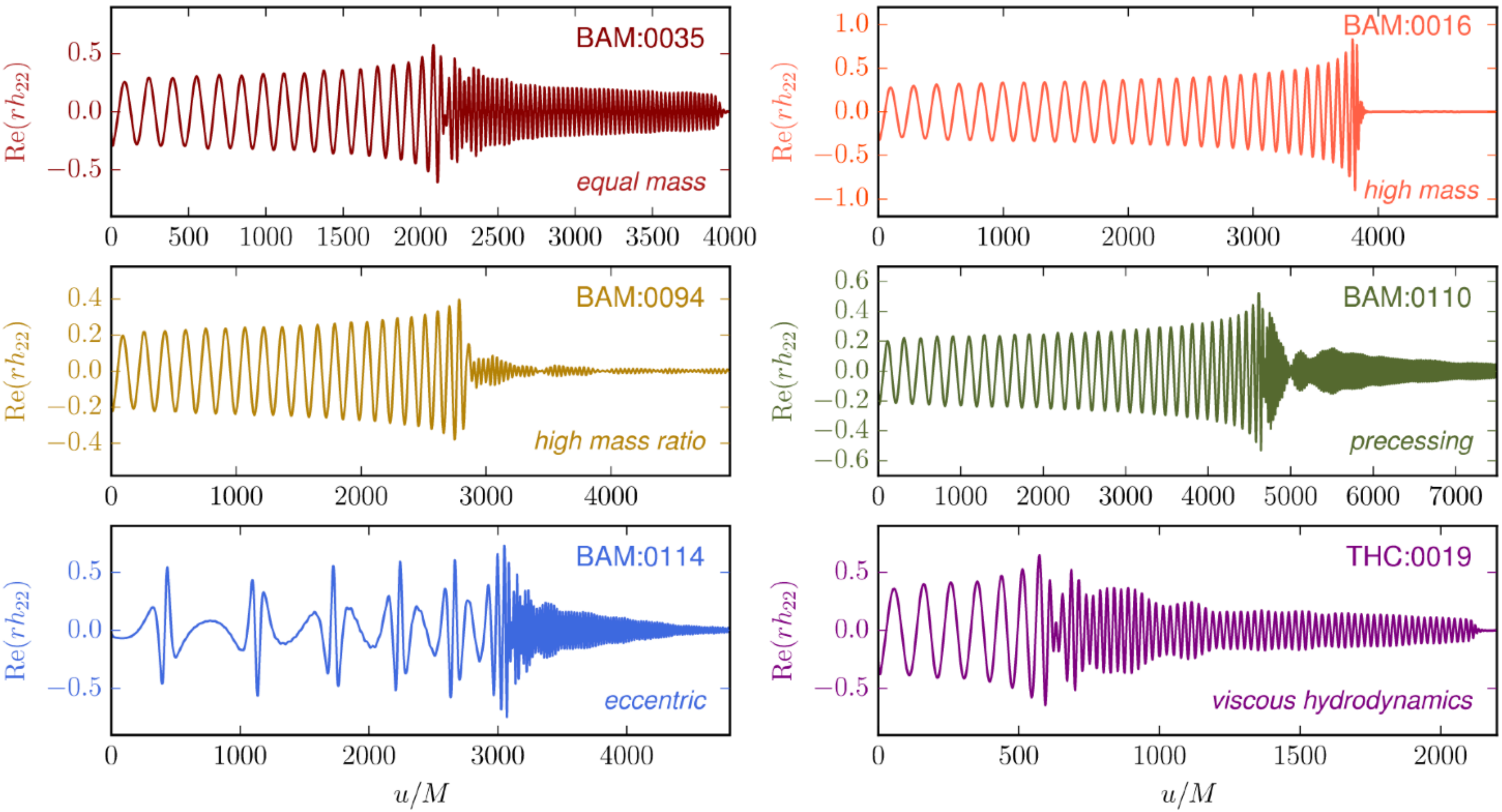

Dietrich+ 2018

Post-Newtonian framework

No exact solution of Einstein's field equations known for the relativistic two-body problem.

Alternatives: perform an **iterative procedure** to obtain corrections to the Newtonian dynamics (**post-Newtonian** expansion), and corrections to flat spacetime accounting for the emission of GWs (**post-Minkowskian** expansion).

Large body of work, in particular for **QC binaries** in the adiabatic approximation (see Blanchet 2014).

PN dynamics: the e.o.m. for each body (non-spinning) in PN theory can be expressed as a power-series in $1/c$ for the acceleration of each body:

$$\frac{d\mathbf{v}_1}{dt} = \mathbf{A}_1^{\mathrm{N}} + \frac{1}{c^2}\mathbf{A}_1^{1\mathrm{PN}} + \frac{1}{c^4}\mathbf{A}_1^{2\mathrm{PN}} + \frac{1}{c^5}\mathbf{A}_1^{2.5\mathrm{PN}} + \frac{1}{c^6}\mathbf{A}_1^{3\mathrm{PN}} + \frac{1}{c^7}\mathbf{A}_1^{3.5\mathrm{PN}} + \frac{1}{c^8}\mathbf{A}_{1,\mathrm{conserv}}^{4\mathrm{PN}} + \mathcal{O}\left(\frac{1}{c^8}\right)$$

n-PN order is the contribution with $1/c^{2n}$ (radiation-reaction starts at 2.5 PN)

Post-Newtonian framework

Most binary systems are expected to have **circularized** by the time the enter the detectors frequency band. Thus, they follow QC orbits in which the radial variation is only due to the energy loss in form of gravitational radiation.

The orbital frequency at a given radius $\Omega = \frac{v}{r}$ can be obtained as a PN series in terms of parameter $\gamma = \frac{GM}{rc^2}$

(known at 4PN order)

$$
\begin{aligned}
\Omega^2 = \frac{GM}{r^3}\Bigg[& 1 + (-3+\eta)\gamma + \left(6 + \frac{41}{4}\eta + \eta^2\right)\gamma^2 \\
& + \left(-10 + \left[-\frac{75707}{840} + \frac{41}{64}\pi^2 + 22\ln\left(\frac{r}{r_0'}\right)\right]\eta + \frac{19}{2}\eta^2 + \eta^3 \right)\gamma^3 \\
& + \left(15 + 48\ln\left(\frac{r_0'}{r_0''}\right) + \eta\left[\frac{19644217}{33600} + \frac{163\pi^2}{1024} + \frac{256}{5}\gamma_E + \frac{128}{5}\ln(16\gamma) \right.\right. \\
& \left. + 82\ln\left(\frac{r_0}{r_0'}\right) - 372\ln\left(\frac{r_0}{r_0''}\right)\right] + \eta^2\left[\frac{44329}{336} - \frac{1907}{64}\pi^2 - \frac{992}{3}\ln\left(\frac{r_0}{r_0'}\right)\right. \\
& \left.\left. + 720\ln\left(\frac{r_0}{r_0''}\right)\right] + \frac{51}{4}\eta^3 + \eta^4 \right)\gamma^4 + \mathcal{O}(\gamma^5)\Bigg],
\end{aligned}
$$

$$\eta = \frac{M_1 M_2}{(M_1+M_2)^2}$$

Post-Newtonian framework

The **binding energy** of quasi-circular orbits can also be computed at 4PN order, in terms of the parameter

$$x = \left(\frac{GM\Omega}{c^3}\right)^{2/3}$$

$$\begin{aligned}
E = -\frac{\eta c^2 x}{2}\Bigg\{ & 1 + \left(-\frac{3}{4} - \frac{\eta}{12}\right)x + \left(-\frac{27}{8} + \frac{19\eta}{8} - \frac{\eta^2}{24}\right)x^2 \\
& + \left[-\frac{675}{64} + \left(\frac{34445}{576} - \frac{205\pi^2}{96}\right)\eta - \frac{155\eta^2}{96} - \frac{35\eta^3}{5184}\right]x^3 \\
& + \left[-\frac{3969}{128} + \left(-\frac{123671}{5760} + \frac{9037\pi^2}{1536} + \frac{1792}{15}\ln 2 + \frac{896\gamma_E}{15}\right)\eta \right. \\
& \left. + \left(-\frac{498449}{3456} + \frac{3157\pi^2}{576}\right)\eta^2 + \frac{301\eta^3}{1728} + \frac{77\eta^4}{31104}\right]x^4 \\
& + \mathcal{O}\left(\frac{1}{c^{10}}\right)\Bigg\}.
\end{aligned}$$

Post-Newtonian framework

In the Post-Minkowskian approximation **gravitational waves** can be expressed as

$$h_+ - ih_\times = \sum_{l=2} \sum_{m=-l}^{l} h_{lm} \; {}^{-2}Y_{lm}(\theta, \phi)$$

where the individual spherical harmonics can be computed from the radiative multipole moments of mass-type and current-type

$$h_{lm} = -\frac{G}{\sqrt{2}Rc^{l+2}}(U_{lm} - \frac{i}{c}V_{lm})$$

Modes can be factorized as $h^{lm} = \frac{2GM\eta x}{Rc^2}\sqrt{\frac{16\pi}{5}}\mathscr{H}^{lm}e^{-im\psi}$

where $\mathcal{H}^{lm}(t)$ are complex amplitude functions and ψ is a phase variable that takes into account distortion due to tail effects. It can be written as

$$\psi = \phi - \frac{2GM\Omega}{c^3}\ln\left(\frac{\Omega}{\Omega_0}\right)$$

where ϕ is the orbital phase and Ω_0 is the orbital frequency at the initial time.

Post-Newtonian framework

For the dominant quadrupole mode *l=m=2*, results are known at 3.5PN beyond the Newtonian order of the quadrupole formula (Faye+ 2012):

$$
\begin{aligned}
\mathscr{H}^{22} = {} & 1 + x\left(-\frac{107}{42} + \frac{55}{42}\eta\right) + 2\pi x^{3/2} + x^2\left(-\frac{2173}{1512} - \frac{1069}{216}\eta + \frac{2047}{1512}\eta^2\right) \\
& + x^{5/2}\left(-\frac{107\pi}{21} - 24i\eta + \frac{34\pi}{21}\eta\right) + x^3\left[\frac{27027409}{646800} - \frac{856}{105}\gamma_E + i\frac{428\pi}{105}\right. \\
& \left. + \frac{2\pi^2}{3} + \left(-\frac{278185}{33264} + \frac{41\pi^2}{96}\right)\eta - \frac{20261}{2772}\eta^2 + \frac{114635}{99792}\eta^3 - \frac{428}{105}\ln(16x)\right] \\
& + x^{7/2}\left[-\frac{2173\pi}{756} + \left(-\frac{2495\pi}{378} + i\frac{14333}{162}\right)\eta + \left(\frac{40\pi}{27} - i\frac{4066}{945}\right)\eta^2\right].
\end{aligned}
$$

The *l=m=3* and *l=3, m=1* subdominant modes are also known at 3.5PN order while the rest of modes are known at 3PN order.

Post-Newtonian framework

The **gravitational energy flux** (energy carried by GW) can be computed from the radiative multiple moments, and is also known at 3.5PN (plus the term at 4.5PN)

$$
\begin{aligned}
\mathscr{F} = \frac{32c^5}{5G}\eta^2 x^5 \Bigg\{ & 1 + \left(-\frac{1247}{336} - \frac{35\eta}{12}\right)x + 4\pi x^{3/2} \\
& + \left(-\frac{44711}{9072} + \frac{9271\eta}{504} + \frac{65\eta^2}{17}\right)x^2 + \left(-\frac{8191}{672} - \frac{583\eta}{24}\right)\pi x^{5/2} \\
& + \left[\frac{6643739519}{69854400} + \frac{16\pi^2}{3} - \frac{1712\gamma_E}{105} - \frac{856}{105}\ln(16x)\right. \\
& \left. + \left(-\frac{134543}{7776} + \frac{41\pi^2}{48}\right)\eta - \frac{94403\eta^2}{3024} - \frac{775\eta^3}{324}\right]x^3 \\
& + \left(-\frac{16285}{504} + \frac{214745\eta}{1728} + \frac{193385\eta^2}{3024}\right)\pi x^{7/2} \\
& + (\text{unknown coefficients})x^4 + \left[\frac{265978667519}{745113600} - \frac{6848}{105}\gamma_E - \frac{3424}{105}\ln(16x)\right. \\
& \left. + \left(\frac{2062241}{22176} + \frac{41\pi^2}{12}\right)\eta - \frac{133112905}{290304}\eta^2 - \frac{3719141}{38016}\eta^3\right]\pi x^{9/2} + \mathscr{O}(x^5)\Bigg\}.
\end{aligned}
$$

Faye+ (2012)
Marchand+ (2017)

Post-Newtonian framework

For **quasi-circular binaries** we need to evaluate the evolution of the orbital frequency (or the PN parameter *x*). For QC binaries the evolution is **adiabatic** and only the **energy balance** is needed:

$$\frac{dE}{dt} = -\mathscr{F}$$ [variation of binding energy of the orbit = - gravitational energy flux]

For eccentric orbits an additional balance equation has to be satisfied by the total angular momentum of the system.

The balance equation and the chain rule allow to obtain the **evolution of the orbital frequency (or *x*)** and thus the **evolution of the orbital phase**:

$$\frac{dx}{dt} = -\frac{\mathscr{F}(x)}{dE/dx}, \qquad \frac{d\phi}{dt} = \frac{x^{3/2}}{M}$$

Different ways of handling these evolution equations lead to different approximants to evolve adiabatic QC compact binaries, usually called **Taylor approximants**. (see Buonanno+ (2009) for a review)

Post-Newtonian framework

`TaylorT1`: result of evolving previous two equations directly using the expressions for the binding energy and for the gravitational flux.

`TaylorT4`: result of re-expanding as a Taylor series in *x* the quotient in the r.h.s. of first equation, and evolving.

`TaylorT2`: analytical expressions for the phase and for the relation between time and frequency can be obtained by inverting the relation

$$\frac{dt}{dx} = -\frac{dE/dx}{\mathscr{F}(x)}$$

and re-expanding the quotient as a Taylor series, since *t(x)* can be integrated directly as a function of *x*:

$$\begin{aligned} t_{3.5}(x) = t_{\rm ref} - \frac{1}{x}\Bigg[& 1 + \left(\frac{743}{252} + \frac{11\eta}{3}\right)x - \frac{32}{5}\pi x^{3/2} + \left(\frac{3058673}{508032} + \frac{5429}{504}\eta \right. \\ & \left. + \frac{672}{72}\eta^2\right)x^2 - \left(\frac{7729}{252} - \frac{13}{3}\eta\right)\pi x^{5/2} + \Bigg\{ -\frac{10052469856691}{23471078400} + \frac{128}{3}\pi^2 \\ & + \frac{6848}{105}\gamma_E + \left(\frac{3147553127}{3048192} - \frac{451}{12}\pi^2\right)\eta - \frac{15211}{1728}\eta^2 + \frac{25565}{1296}\eta^3 \\ & + \frac{3424}{105}\ln(16x)\Bigg\}x^3 + \left(-\frac{15419335}{127008} - \frac{75703}{756}\eta + \frac{14809}{378}\eta^2\right)\pi x^{7/2}\Bigg]. \end{aligned}$$

Post-Newtonian framework

Using the chain rule the orbital phase can be expressed as

$$\frac{d\phi(x)}{dx} = \frac{d\phi(x)}{dt}\frac{dt}{dx} = x^{3/2}\frac{dt}{dx}$$

which can be integrated analytically using the previous expression for $t_{3.5}(x)$

$$\begin{aligned}\phi_{3.5}(x) = \phi_{\rm ref} - \frac{1}{x}\Bigg[1 &+ \left(\frac{3715}{1008} + \frac{55\eta}{12}\right)x - 10\pi x^{3/2} + \left(\frac{15293365}{1016064} + \frac{27145}{1008}\eta\right. \\ &\left.+ \frac{3085}{144}\eta^2\right)x^2 + \left(\frac{38645}{672} - \frac{65\eta}{8}\right)\ln(6x^{1/2})\pi x^{5/2} + \Bigg\{\frac{12348611926451}{18776862720} \\ &- \frac{160}{3}\pi^2 - \frac{1712}{21}\gamma_E + \left(\frac{2255}{48}\pi^2 - \frac{15737765635}{12192768}\right)\eta + \frac{76055}{6912}\eta^2 \\ &- \frac{127825}{5184}\eta^3 - \frac{856}{21}\ln(16x)\Bigg\}x^3 + \left(\frac{77096675}{2032128} + \frac{378515}{12096}\eta\right. \\ &\left.- \frac{74045}{6048}\eta^2\right)\pi x^{7/2}\Bigg].\end{aligned}$$

TaylorT3: constructed by inverting the relation *t(x)* order by order in the Taylor expansion. This provides an analytical series expression for *x(t)* that can be integrated analytically to obtain $\phi(t)$.

Post-Newtonian framework

For data analysis it is important to have the GW signal in the **frequency domain**. In the stationary phase approximation the Fourier transform reads:

$$\tilde{h}(f) \approx \tilde{h}^{\mathrm{SPA}}(f) = \frac{A(t_f)}{\sqrt{\ddot{\phi}(t_f)}} e^{i(2\pi f t_f - 2\phi(t_f) - \pi/4)}$$

Fourier domain phase $\psi_f(t_f) = 2\pi f t_f - 2\phi(t_f)$

$\psi(f)$ can be found evaluating the `TaylorT2` approximant for $t_{3.5}(x)$ at $x_f = (GM\pi f/c^3)^{2/3}$ to obtain $t(f)$.

The Fourier domain phase satisfies a differential equation $\dfrac{d\psi(f)}{df} = 2\pi t(f)$

that can be integrated analytically in f to provide the `TaylorF2` approximant.

`TaylorF2` approximant widely used: (1) fast closed-form expressions for Fourier-domain templates for DA; (2) starting point for building phenomenological Fourier-domain models.

Post-Newtonian framework

Spinning binaries: spins introduce three intrinsic degrees of freedom in the bodies. Spin effects are typically characterized in the pole-dipole approximation of Papapetrou (1951) through the introduction of an antisymmetric tensor in the energy-momentum tensor of the bodies. This tensor can be expressed in terms of the spatial spin vectors of each body.

Contributions from the spins to the dynamics:

- Leading-order: Spin-orbit (SO) interaction with the orbital angular momentum of the binary. Enters at 1.5PN order.
- Next effect: spin-spin (SS) interactions. Enter at 2PN order.

Contributions from the spins to the energy flux computed at 4PN for QC orbits for the SO interaction (Blanchet+ 2006, Bohé+ 2013, Marsat+ 2014) and 3PN for the SS interaction (Bohé+ 2015).

Strategy: the different spin contributions can be added to the non-spinning binding energy and energy flux and propagated to the different Taylor approximants.

Post-Newtonian framework

Precessional motion: through interactions of the individual spins with the orbital angular momentum and themselves, the orientation of the spins and the orientation of the orbital angular momentum, follow evolution equations

$$\frac{d\hat{\boldsymbol{L}}}{dt} = \boldsymbol{\Omega}_{\hat{L}}(\boldsymbol{L}, \boldsymbol{S}_1, \boldsymbol{S}_2) \times \hat{\boldsymbol{L}},$$
$$\frac{d\boldsymbol{S}_1}{dt} = \boldsymbol{\Omega}_1(\boldsymbol{L}, \boldsymbol{S}_1, \boldsymbol{S}_2) \times \boldsymbol{S}_1$$
$$\frac{d\boldsymbol{S}_2}{dt} = \boldsymbol{\Omega}_2(\boldsymbol{L}, \boldsymbol{S}_1, \boldsymbol{S}_2) \times \boldsymbol{S}_2$$

(credit: F. Ohme)

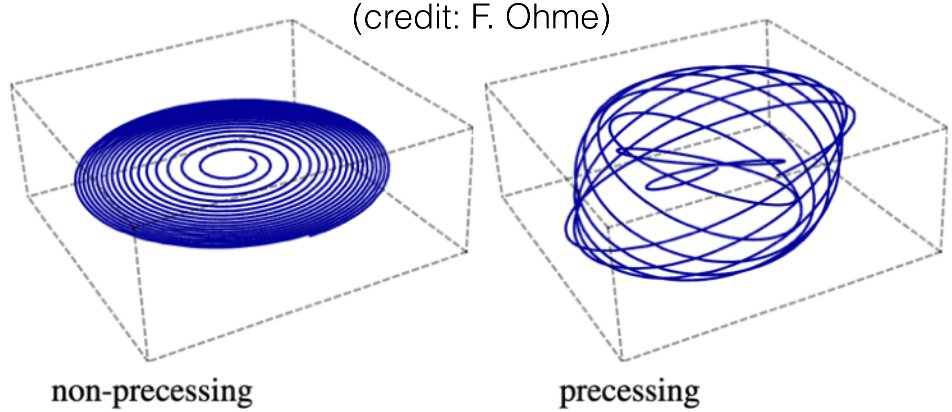

where the precessing frequencies $\boldsymbol{\Omega}_a$ depend on the individual spins and on the orbital angular momentum of the binary.

For precessional motion the GW polarizations can contain **complicated modulations**, since angle between line-of-sight and orbital plane varies with time.

A framework to approximately **demodulate** the precessing effects in the spherical harmonic modes was developed by Schmidt+ (2011, 2012, 2015) - the **"twisting-up" approximation**.

Post-Newtonian framework

Idea: the source multipoles that generate the GW seem to precess with the orbital plane. Define a non-inertial frame aligned with the orbital plane or the direction of maximum GW emission - **co-precessing frame** or quadrupole-aligned frame.

With respect to this frame, the spherical harmonic decomposition provides modes that are **demodulated** from precessional effects. Modes in this frame can be **approximately mapped** to the modes of an equivalent non-precessing binary

$$h_{lm}^{\mathrm{coprec}}(t;\eta,\boldsymbol{\chi}_1,\boldsymbol{\chi}_2) \approx h_{lm}^{\mathrm{AS}}(t;\eta,\chi_{1l},\chi_{2l})$$

$\chi_{il} = \mathbf{S}_i \cdot \mathbf{L}/m_i^2$ are the equivalent aligned dimensionless spins.

The transformation from the co-precessing frame to an inertial frame is required for the description of the polarization at the detectors. It corresponds to an instantaneous Euler rotation.

$$h_{lm}(t) = \underbrace{\mathscr{D}^{l}_{mm'}}_{\text{Wigner-D matrix}}(\underbrace{\alpha,\beta,\gamma}_{\text{Euler angles}})h_{lm'}(t)$$

Closed-formed approximations to the angles implemented in “twisted-up” Phenom models. Numerical evolution of angles implemented in EOB-based models and interpolated expressions from NR simulations employed in NRSurrogate models.

Effective One Body approach (see Alessandro's talk)

EOB is another approach to describe the two-body dynamics in GR and its GW emission. Based on a **resummation** of the PN information for the dynamics in terms of the geodesic motion of a particle in an **effective spacetime**. Started with the seminal work of Buonanno and Damour (1999, 2000).

EOB provided first qualitative predictions of the plunge and merger of BBH systems before the NR breakthroughs.

Idea: map the two-body problem into the effective problem of a particle of mass μ in an effective spacetime which is a symmetric deformation of Schwarzschild (or Kerr for spinning binaries).

$\mu = M_1 M_2 / M$ (reduced mass of binary system)

Mapping performed in terms of matching the energy levels of the Hamiltonian operators describing both systems.

The dynamics in the center-of-mass frame $\mathbf{p}_1 = -\mathbf{p}_2$ at 3PN order are encoded in a Hamiltonian

$$H^{\rm rel}(\mathbf{q},\mathbf{p}) = \frac{\mathbf{p}^2}{2\mu} - \frac{GM\mu}{|\mathbf{q}|} + \frac{1}{c^2}H_2(\mathbf{q},\mathbf{p}) + \frac{1}{c^4}H_4(\mathbf{q},\mathbf{p}) + \frac{1}{c^6}H_6(\mathbf{q},\mathbf{p}) + \mathscr{O}\left(\frac{1}{c^8}\right)$$

Effective One Body approach

Conservative dynamics of the two-body system encoded in the **EOB Hamiltonian.** Latter obtained by starting with a spherically symmetric spacetime that depends on the symmetric mass ratio of the system (and approaches Schwarzschild in the test-particle limit) and by requiring that the dynamics of the particle satisfy the Hamilton-Jacobi equation.

The EOB Hamiltonian can be written as

$$\frac{1}{\mu} H_{\rm EOB}(r, p_{r*}, \phi, p_\phi) \equiv \hat{H}_{\rm EOB} = \frac{1}{\eta}\sqrt{1 + 2\eta(\hat{H}_{\rm eff} - 1)}$$

where the effective Hamiltonian depends on the canonical momenta p_{r^*}, p_ϕ

From the EOB Hamiltonian the evolution of the phase space variables can be obtained through the Hamilton e.o.m.

For quasi-circular orbits in the equatorial plane and assuming that radiation-reaction enters only through a tangential force $\mathcal{F}_\phi$, the equations are:

Effective One Body approach

Evolution equations:

$$\frac{d\phi}{dt} = \frac{\partial \hat{H}_{\rm EOB}}{\partial p_\phi},$$
$$\frac{dr}{dt} = \sqrt{\frac{A}{B}}\frac{\partial \hat{H}_{\rm EOB}}{\partial p_{r*}},$$
$$\frac{dp_\phi}{dt} = \hat{\mathscr{F}}_\phi,$$
$$\frac{dp_{r*}}{dt} = -\sqrt{\frac{A}{B}}\frac{\partial \hat{H}_{\rm EOB}}{\partial r}.$$

A and *B* are metric potentials of the underlying spherically symmetric spacetime.

The tangential radiation-reaction force can be associated with the GW flux *F*:

$$\mathscr{F}_\phi \equiv -\frac{1}{\Omega}F$$

$\Omega = \dot{\phi}$ is the angular orbital frequency of the system

First attempts to construct a resummed version of the flux incorporating test-particle results at higher order (to improve the accuracy of known PN results) were taken by Damour+ (1998).

Effective One Body approach

A **different strategy** for describing the GW flux based on a resummation framework for the GW amplitudes was initiated by Damour and Nagar in 2008. Many papers followed …

Idea: GW spherical harmonics of a QC non-precessing BBH system factorized as

Tail effects

High-order tail effects

Relativistic amplitudes (factored-out)

$$h_{lm}(x) = h_{lm}^{(N,\epsilon)} T_{lm} e^{i\delta_{lm}} \hat{S}_{\rm eff}^{(\epsilon)} f_{lm}(v;\eta,\chi_1,\chi_2)$$

Newtonian pre-factor

Effective source term (energy flux / angular momentum flux)

$\epsilon = l + m$

Mode parity

Amplitudes f_{lm} improved through resummation in Nagar & Shah (2016)

Comparison with NR simulations and test-particle results **outperform** the standard Taylor-expanded form (Messina+ 2018, Nagar+ 2019).

The GW flux (the tangential force) obtained from the expression of the asymptotic instantaneous circular flux:

$$\mathscr{F}_\phi = -\frac{1}{\Omega}\frac{2}{16\pi G}\sum_{l=2}^{l_{\rm max}}\sum_{m=1}^{l}(m\Omega)^2|rh_{lm}|^2.$$

Effective One Body approach - merger-ringdown attachment

Buonanno & Damour (1999): full waveform described by an EOB inspiral-plunge waveform plus a merger-ringdown waveform, joined at time of merger (peak of orbital frequency):

$$h_{lm}^{\mathrm{EOB}}(t) = \theta(t_m - t)h_{lm}^{\text{insp-plunge}}(t) + \theta(t - t_m)h_{lm}^{\mathrm{RD}}(t)$$

First attempt to add a merger-ringdown continuation based on a superposition of QNM states whose ringdown and damping frequencies can be obtained from BH perturbation theory (depend on final mass and spin of remnant BH).

Improvements done by fitting remnant quantities to results from NR simulations.

Damour & Nagar (2014): factorizing the QNM superposition as the longest-lived, ground state mode (n=1) and the rest of the superposition:

$$\bar{h}_{lm}(\tau) \equiv e^{\sigma_{1,l,m}\tau} h_{lm}(\tau) \qquad\qquad \tau = t_m - t$$

Phenomenological expressions proposed for residual waveform, in terms of its amplitude and phase. Approach currently employed in state-of-the-art waveform models based on the EOB framework.

IMR waveform models - SEOBNR family (AEI)

Increase in available NR simulations after 2005 allowed to calibrate the EOB Hamiltonian, with gradual improvements.

- Buonanno+ (2007): 4PN contribution added to the A metric potential (conservative sector).
- Buonanno+ (2009): non-quasicircular corrections to the radiative sector, calibrated to an equal-mass, nonspinning, NR simulation.
- Pan+ (2010): as Buonanno+ (2009) but calibrated for a set of equal-mass, spinning, non-precessing NR simulations.
- Pan+ (2011): non-quasicircular corrections to HM calibrated for unequal-mass, nonspinning simulations.
- Taracchini+ (2014): model for generic spins and mass ratio, `SEOBNRv3`. Accurate enough to perform PE of the first GW detection, GW150914.
- Bohé+ (2017): drastic update in accuracy for the dominant mode for aligned-spin configurations, `SEOBNRv4`.
- Cotesta+ (2018): subdominant modes, aligned-spin configurations, `SEOBNRv4HM`.
- Ossokine+ (2020): generic spin configurations, `SEOBNRv4P`, `SEOBNRv4PHM`.

IMR waveform models - TEOBResumS family (Jena+Torino)

New EOB framework based on the concept of centrifugal radius, new resummation techniques, and a self-consistent radiation-reaction force.

- Nagar+ (2018): Initial model, dominant mode.
- Nagar+ (2020a): higher-order multipoles, non spinning systems.
- Nagar+ (2020b): higher-order multipoles, aligned-spin systems.
- Ackay+ (2021): precessing systems.

QC orbits

- Chiaramello & Nagar (2020): moderately **eccentric** orbits.
- Nagar+ (2021): generic orbits, including hyperbolic encounters.

Last model employed by Gamba+ (2021) in the analysis of GW190521 as a dynamical capture event.

(see talk by Rossella on the status of TEOBResumS)

IMR waveform models - Phenom family

Initial idea: provide a **Fourier-domain template bank** for GW detection based on NR simulations. Initiated by Jena+AEI and further developed by Cardiff and UIB.

- Ajith+ (2008): analytical model based on `TaylorF2` and a phenomenological ansatz for the MR (inspired on QNM behaviour) calibrated with non spinning simulations, `IMRPhenomA`.
- Ajith+ (2011): phenomenological part calibrated with aligned-spin simulations, `IMRPhenomB`.
- Santamaría+ (2010): accurate hybrid waveforms constructed employing PN for inspiral and attaching non-precessing NR simulations. Then, analytical Fourier-domain formula for the dominant mode constructed and coefficients calibrated to the simulations. Model `IMRPhenomC`.

  Main innovation: Fourier-domain phase split into three regions with the transitions smoothened by tanh-window functions:

$$\psi_{\rm phen}(f) = \psi_{\rm TF2} w^{-}_{f_1} + \psi_{\rm premerge} w^{+}_{f_1} w^{-}_{f_2} + \psi_{\rm RD} w^{+}_{f_2}$$

- Schmidt+ (2012, 2015): extension of the previous model to generic spin configuration, in the "twisting-up" framework, `IMRPhenomP`.

IMR waveform models - Phenom family

- Khan+ (2016): `IMRPhenomD`. Several improvements w.r.t. `IMRPhenomC`:

  Phase of dominant mode split in 3 regions; inspiral part still modelled by `TaylorF2` but adding 5 extra PN coefficients at higher orders, calibrated to NR simulations. Similarly done for the amplitude.

  MR part improved with a Lorentzian-like ansatz based on QNM behavior in the Fourier domain.

- Bohé+ (2016): `IMRPhenomPv2`. Adaptation of `IMRPhenomP` to the improvements of `IMRPhenomD`. It was one of the most employed waveform models during O1, O2 and O3b.

- Khan+ (2019): Implementation of multi-scale analysis precessing angles (Chatziioannou+ 2017) led to `IMRPhenomPv3`.

- Khan+ (2020): Inclusion of the effects of subdominant harmonics: `IMRPhenomHM` and `IMRPhenomPv3HM`. First spinning multimode models available for QC binaries. Employed in the analysis of the first confident mass-asymmetric binary reported by the LVK, GW190412.

IMR waveform models - Phenom family

The UIB group pursued a different strategy: from the start NR information included on the same footing for the dominant *and* subdominant modes. Led to the `PhenomX` family.

- Pratten+ (2020): `IMRPhenomXAS`. New model for the dominant mode (similar ansatz strategy than for `IMRPhenomD`). Improved over **2 orders of magnitude** the accuracy of `IMRPhenomD` model (collocation points used instead of calibrating phenomenological coefficients).

- García-Quirós+ (2020): extension to higher modes, `IMRPhenomXHM`. Drastic improvement over `IMRPhenomHM`. Resolved previous tensions found for GW190412 (Colleoni+ 2021).

- Pratten+ (2021): generic spin systems, `IMRPhenomXP` and `IMRPhenomXPHM`.

Complementary **time-domain route** followed in the PhD thesis of H. Estellés:

- Estellés+ (2021): dominant mode, aligned spins, `IMRPhenomT`.
- Estellés+ (2022a): subdominant modes, aligned spins, `IMRPhenomTHM`.
- Estellés+ (2022b): subdominant modes, generic spins, `IMRPhenomTPHM`.

IMR waveform models - NRSurrogate family

Surrogate models: “Brute-force” approach to <u>efficiently</u> generate waveforms with accuracy comparable to NR.

Idea outlined in Field+ (2014) for a fast surrogate of non spinning EOB waveforms:

- Select the most relevant m points in the parameter space of WFs (greedy algorithm, tolerance error from inner product of WFs).
- Express WFs as a sum of m reduced basis elements, by selecting m empirical nodes.
- Perform a parameter fit of each node across the parameter dimension.
- Evaluate model for any parameter value using amplitude and phase fits at each empirical node.

Blackman+ (2015): surrogate model for non spinning simulations up to $q=8$. Proof-of-concept that surrogate models could achieve greater accuracy than semi-analytical models like SEOB.

Blackman+ (2017): first NR surrogate model for precessing systems, `NRSur4ds2` (based on a rotation to a co-precessing frame and back; as done in the analytical models). Harmonic content limited to $l=3$ and mass-ratio to $q=2$.

IMR waveform models - NRSurrogate family

Varma+ (2019): `NRSur7dq4`.

Calibrated with 1528 NR precessing simulations up to $q=6$ and spin magnitudes up to 0.8, covering harmonic content up to $l=4$ and retaining the full 7 intrinsic degrees of freedom of QC BBH systems.

`NRSur7dq4` is the **most accurate WF model** for QC BBH systems with generic spins to date.

It has been employed:

- In several exceptional event papers from the LVK collaboration (GW190412, GW190521)
- in studies of spin distribution in the BBH population (Varma+ 2022)
- in the first confident identification of a precessing binary, GW200129 (Hannam+ 2021)

BBH GW modelling - Alternatives?

Machine Learning can help complete template banks, aid searches and PE:

- **WF modelling**: Gaussian Process Regression used to build WF surrogate models of both non-precessing and precessing BBH systems at points of the parameter space not covered by NR (Williams+ 2020).

- **BBH searches**: CNN used to search for BBH GW signals. Tests using whitened time series of measured GW strain in Gaussian noise. Sensitivity comparable to matched filtering (Gabbard+ 2018, George & Huerta 2018).

  The 1st ML GW search mock data challenge (Schäfer+ 2022): competitive on simulated data; struggle to handle real noise and identify long-duration signals.

- **Rapid inference of source properties**: likelihood-free, autoregressive normalizing flows yield performance comparable to MCMC (Green+ 2020); conditional variational autoencoders perform full PE on GW150914 in ~1s (Gabbard+ 2022).

CBC GW modelling - current frontier

Aspects to improve:

- increase mass ratio and harmonic content
- decrease WF systematics
- **models for non-QC binaries** (eccentricity, dynamical captures, hyperbolic encounters)

  Increasing effort from EOB, NRSurrogate and Phenom WF families on modelling eccentric, non-precessing BBH with higher order modes: Nagar+ 2021, Liu+ 2021, Khalil+ 2021, Albanesi+ 2021, Islam+ 2021, Ramos-Buades+ 2021, 2022

  [see talks by Alessandro, Gonzalo, Rossella, Simone and Tomás; see also talk by Mark on astrophysical rates and populations]

- WF models for exotic compact objects? [see talks by Juan and Nico]
- WF models beyond GR?

Non-vanilla detections to become more common

Absence of pre-merger emission in GW190521 hampers interpretation of the source (influence of priors)

LVC
PRL, 125, 101102 (2020)

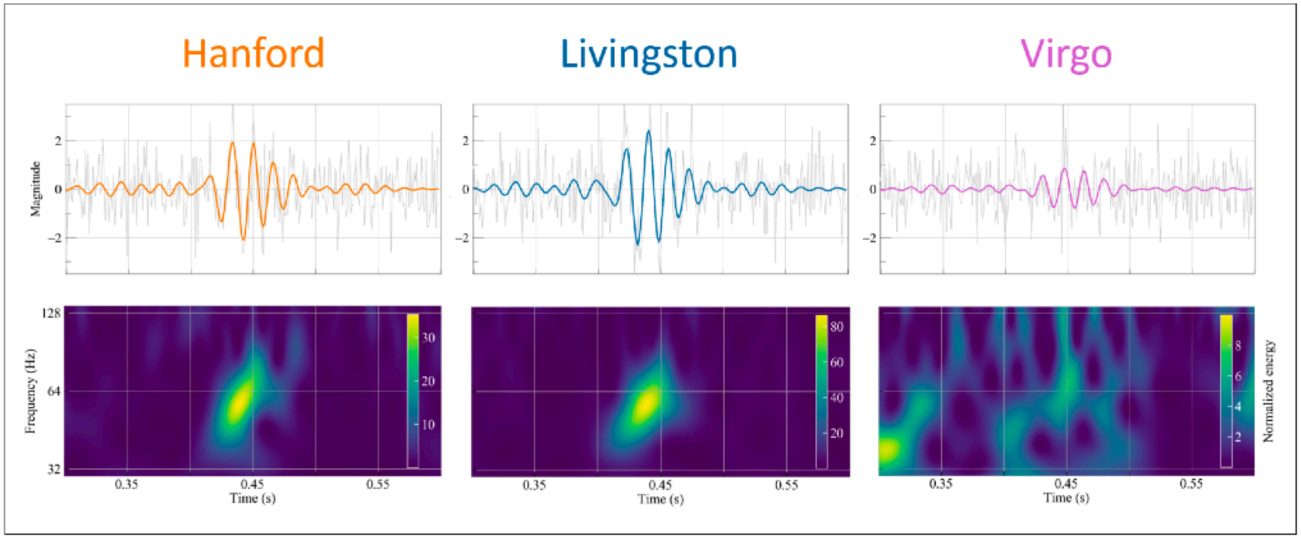

Interpretations involving BH mergers:

- LVK: quasi-circular BBH merger, precession, primary mass in PISN gap
- Romero-Shaw+ 2020: weakly eccentric BBH merger
- Fishbach+ 2020: straddling binary
- Gamba+ 2021; dynamical encounter
- Gayathri+ 2022: highly eccentric BBH merger

Other proposals:

- Calderón-Bustillo+ 2021: collisions of boson stars
- De Luca+ 2021: PBH origin
- Shibata+ 2021: high-mass disk-BH system
- Palmese+ 2021: merger of ultradwarf galaxies
- …

The story so far …

The LVK Collaboration has conducted three observing runs. **O4** to start in March 2023 with an expected rate of detections (CBCs) of about **1 per day**.

O5 to follow (sometime in 2026) with **~few per day**.

Likely to boost multimessenger observations.

GWTC-3 contains 90 GW detections, all consistent with CBCs. **Waveform modelling** (analytical and NR) **fundamental**. It has yielded the template banks that have allowed for those detections and the characterization of their sources.

LVK observations

- are unveiling new populations of compact object binaries.
- are impacting many different fields across physics.

Bright future ahead: Multiband GW astronomy across several orders of magnitude in frequency (3G+LISA) will bloom in the next decade.

Extra

BNS mergers

Before merger $(20\,\mathrm{Hz} < \nu <\sim \mathrm{kHz})$

After merger $(\nu >\sim \mathrm{kHz})$

post-Newtonian / EOB

Numerical Relativity

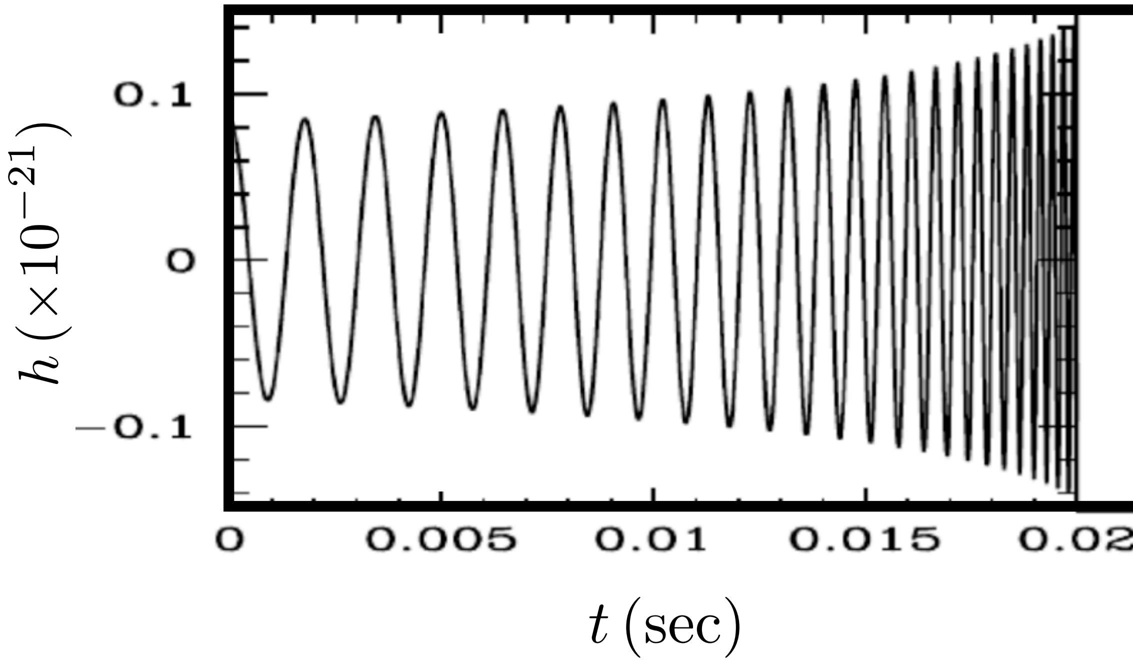

Einstein's gravity

Hydrodynamics/MHD

B-field amplification

Supranuclear matter EoS

Neutrino emission

?

Tidal information incorporated in the approximants

Post-merger waveform is the current frontier

LVK Observing timeline

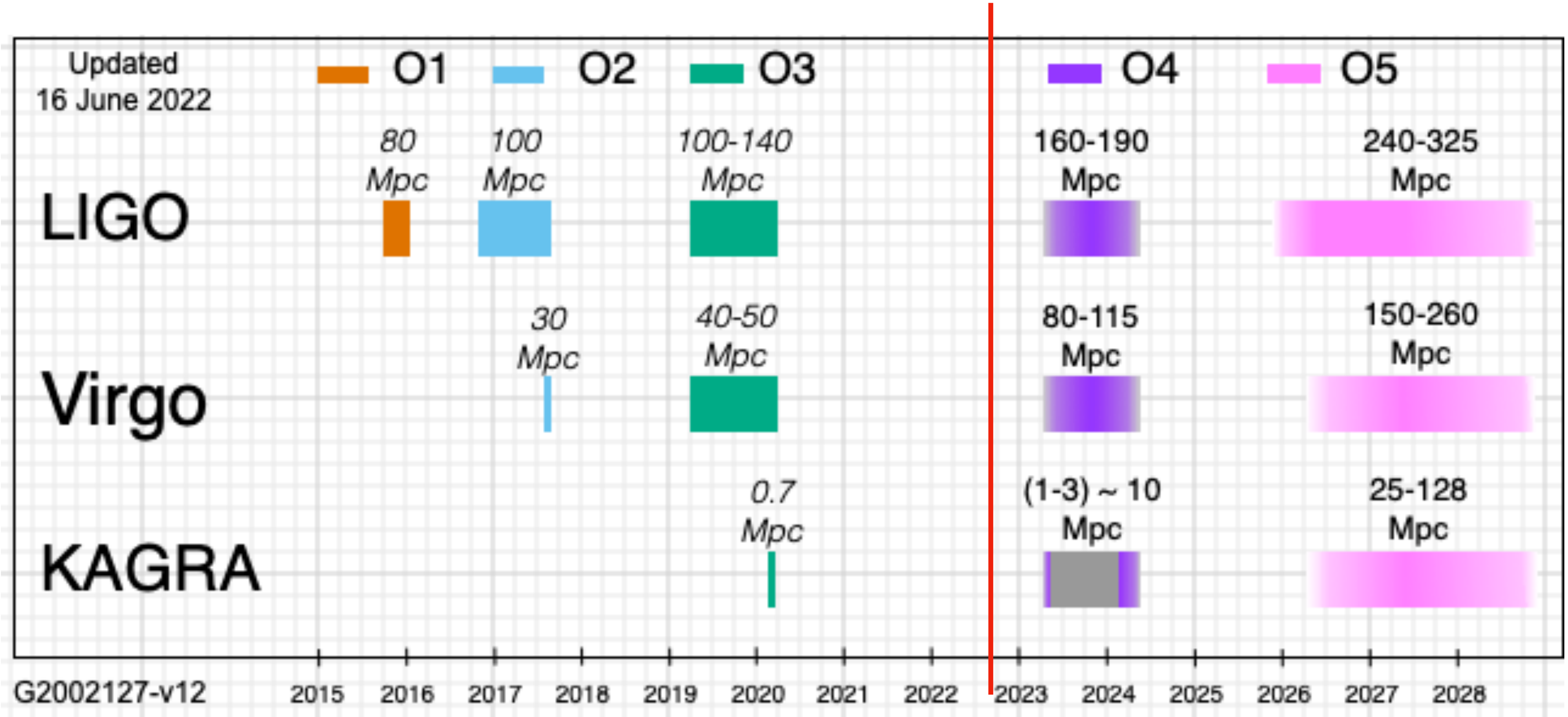

More details at: https://observing.docs.ligo.org/plan/

All data is **public**: Gravitational Wave Open Science Center (www.gw-openscience.org)